Separation Science and Technology
Publication details, including instructions for authors and subscription information:
http://www.informaworld.com/smpp/title~content=t713708471

Lysine Adsorption on Cation Exchange Resin. IV. Temperature Effects on Equilibrium and Kinetics in Batch and Column Systems

Hidetada Nagai[a]; Ko Kuwabara[a]; Giorgio Carta[b]
[a] Fermentation and Biotechnology Laboratories, Ajinomoto, Co., Inc., Kawasaki-shi, Japan [b] Department of Chemical Engineering, University of Virginia, Charlottesville, Virginia, USA

To cite this Article Nagai, Hidetada , Kuwabara, Ko and Carta, Giorgio(2008) 'Lysine Adsorption on Cation Exchange Resin. IV. Temperature Effects on Equilibrium and Kinetics in Batch and Column Systems', Separation Science and Technology, 43: 3, 512 — 532
To link to this Article: DOI: 10.1080/01496390701812459
URL: http://dx.doi.org/10.1080/01496390701812459

Separation Science and Technology, 43: 512–532, 2008

ISSN 0149-6395 print/1520-5754 online
DOI: 10.1080/01496390701812459

Lysine Adsorption on Cation Exchange Resin. IV. Temperature Effects on Equilibrium and Kinetics in Batch and Column Systems

Hidetada Nagai,[1] Ko Kuwabara,[1] and Giorgio Carta[2]

[1]Ajinomoto, Co., Inc., Fermentation and Biotechnology Laboratories, Kawasaki-shi, Japan
[2]Department of Chemical Engineering, University of Virginia, Charlottesville, Virginia, USA

Abstract: Ion exchange equilibria and kinetics are determined for lysine adsorption on the strong acid cation exchanger DIAION SK-1B at temperatures of 25, 40, and 60°C. The ion exchange equilibrium is found to be independent of temperature. Conversely, the kinetics of ion exchange increases dramatically as the temperature is increased. Average ion exchange selectivity coefficients of 6.0 g/cm^3 and 0.52 are obtained for the ion exchange of divalent and monovalent cationic lysine with hydrogen ion, respectively. Resin phase diffusivities are determined by fitting batch binary ion-exchange data with a mass transfer model based on the Nernst-Planck equations. As the temperature is increased from 25 to 60°C, the resin phase diffusivity increases from 0.04×10^{-6} to 0.14×10^{-6} cm^2/s for divalent lysine and from 0.16×10^{-6} to 0.55×10^{-6} cm^2/s for monovalent lysine. The combination of temperature-independent ion exchange equilibria and faster mass transfer at higher temperatures results in higher dynamic binding capacity and more efficient desorption of lysine when ion exchange is operated at an elevated temperature. This behavior is confirmed by means of column adsorption/desorption experiments whose results are found to be in agreement with a model incorporating the equilibrium and mass transfer data obtained in this work.

Keywords: Ion exchange, lysine, equilibrium mass transfer, temperature effects

Received 6 March 2007, Accepted 2 November 2007
Address correspondence to Hidetada Nagai, Ajinomoto, Co., Inc., Fermentation and Biotechnology Laboratories, Kawasaki-ku, Kawasaki-shi, Japan. E-mail: hidetaga_nagai@ajinomoto.com

INTRODUCTION

Ion exchange plays a central role in the industrial production of amino acids and is especially critical in the manufacture of lysine, one of the largest industrial fermentation products (1). Amino acids are amphoteric and can be positively charged, neutral, or negatively charged depending on the solution pH. As a result, amino acids that are bound to a cation exchange resin at low pH can be desorbed by raising the pH to a value where the amino acid becomes negatively charged. For practical and economic reasons, ammonia is often used as a desorbent. Rational design and optimization of such ion exchange processes requires the knowledge of both the ion exchange equilibrium, which determines the maximum resin loading capacity, and the ion exchange kinetics, which determines the dynamic binding capacity as a function of flow rate as well as the time and amount of desorbent required for elution. As a result, a quantitative understanding of these two factors is critical.

In previous work (2, 3), ion exchange equilibria and kinetics were determined for lysine adsorption and desorption on the strong acid cation exchanger Dowex HCR-W2. A model taking into account the speciation of lysine among its different charged forms was also developed to predict lysine adsorption over a broad range of conditions in batch and column systems. The model was further extended to simulate the cyclic adsorption/desorption of lysine in a multicolumn, simulated countercurrent system and the model results were found in excellent agreement with experimental results obtained with an eight-column bench scale system (4).

However, our previous work on lysine ion exchange was conducted entirely at room temperature, while industrial applications are frequently conducted at higher temperatures. This can have multiple practical benefits. For example, lysine solutions concentrated by evaporation at temperatures from 40°C to 60°C are often fed directly to ion exchange columns. Beside the practical advantage of avoiding a cooling step, operation above room temperature may also offer the advantage of faster mass transfer, thus, enhancing the process efficiency. Limited information is available on the ion exchange behavior of amino acids at higher temperatures, although (5) have shown that increasing temperature from 25°C to 85°C has minimal effects on the equilibrium adsorption capacity of phenylalanine while dramatically increasing the resin-phase diffusivity, especially for more highly crosslinked resins. As a result, the dynamic binding capacity, which, in general, depends on both equilibrium and rate, can potentially be increased substantially by operating at higher temperatures.

The objectives of this paper are twofold. The first is to extend our prior measurements of lysine ion exchange equilibrium and rates to higher temperatures. Ion exchange equilibrium constants and resin-phase diffusivities of lysine are obtained for a typical poly(styrene-divinylbenzene) cation exchanger at different temperatures. The second objective is to extend our previously developed model to predict the effect of temperature on

lysine adsorption and desorption in cation exchange columns. The model is validated by comparison with experimental results obtained at the bench scale. Together, these developments provide a way of predicting process performance for lysine ion exchange processes operated at higher temperatures a well as a methodology to extend such predictions to other amino acids.

MATERIALS AND METHODS

The resin used in this work is DIAION SK-1B (Mitsubishi Chemical Co., Tokyo, Japan), a typical gel-type poly(styrene-divinylbenzene) cation exchanger with a nominal DVB content of 8% and sulfonic acid functional groups. The mean particle diameter of the hydrogen form resin is 530 μm as determined from microphotographs. The dry weight of the resin in H-form is 0.465 g dry/g of hydrated particles, while the density of the resin beads in hydrogen form is 0.493 g dry/cm^3. The total ion exchange capacity of the resin is 4.9 ± 0.1 mequiv/g dry H-form resin ($\sim$2.3 mequiv/cm^3-hydrated resin). This value was estimated from the adsorption capacity of monovalent lysine and is in agreement with the specifications of the resin manufacturer. L-lysine was obtained from Ajinomoto Co., Inc. (Raleigh, NC). Ammonium hydroxide and ammonium chloride were from Kanto Chemical Co., Inc. (Tokyo, Japan) and Kishida Chemical Co., Ltd. (Osaka, Japan), respectively.

Ion dissociation equilibria for lysine at different temperatures and ionic strengths were determined from potentiometric titrations as described by (6). Ion exchange equilibria were determined by a batch method as described in (2). Briefly, solutions containing lysine and ammonia were prepared with constant concentrations of chloride ion using stock solutions of lysine hydrochloride, ammonium hydroxide and hydrochloric acid (HCl). Aliquots of these solutions (10 cm^3) were then added to test tubes containing various amounts of wet H-form resin. The tubes were rotated for 4 hours, which was sufficient to reach equilibrium as indicated by batch experiments where the solution concentrations were monitored as a function of time. Temperatures were set at 25°C, 40°C, and 60°C with a thermostatic water bath. The amount of lysine adsorbed by the resin was calculated from the residual composition of the solution phase using a material balance.

HPLC was used to determine the concentrations of ammonia and lysine using a DKK-TOA Co. (Tokyo, Japan) PCI-322 column (4.6 mm I.D. × 250 mm) using a 6 mM aqueous solution of methanesulfonic acid (Wako Junyaku Chemicals, Osaka, Japan) as the mobile phase and detection with a Model ICA-2000 conductivity detector from DKK-TOA Co. (Tokyo, Japan). The injection sample size was 50 μl.

Ion exchange rates were measured in a 100 cm^3 thermostatted glass vessel at 25°C, 40°C, and 60°C as discussed in (2). The vessel is agitated at 300 rpm

with a magnetically driven Teflon impeller, which rests on the vessel's conical bottom preventing damage to the particles while ensuring their complete suspension and mixing of the solution. Samples of solutions containing a selected counterion were added to the vessel and allowed to reach thermal equilibrium. Resin samples were then quickly added and the course of the exchange process monitored by taking 0.5 cm^3 samples and analyzing them by HPLC, as described previously. Ammonium/hydrogen ion exchange kinetics experiments were also followed by continuously monitoring the electrical conductivity of the solution using a Model CM-30G conductivity meter from DKK-TOA Co. (Tokyo, Japan) with a probe dipped in the agitated vessel.

Column experiments were conducted with jacketed glass chromatography columns 2.6 cm in diameter and 5 cm in length (Model XK-26, GE Healthcare, Chicago, IL) packed with a 50% slurry of the resin followed by flow packing. The packed bed density of these columns was 0.49 ± 0.02 g dry resin/cm^3, determined by emptying a packed column and weighing the oven-dried resin. The void fraction was 0.34 ± 0.01, based on pulse injections of blue dextran (MW $>$2,000,000) detected at 280 nm with a Model L-4000H ultraviolet (UV) chromatographic detector from HITACH (Tokyo, Japan). Solutions containing 0.2 M lysine with sulphate concentrations of 0.1, 0.2, or 0.4 M were used as the feed and 1 M ammonium hydroxide as the desorbent, pumped to the column with a HITACHI Model L-6320 intelligent pump. The effluent pH was monitored with a Model HM-30G pH meter and a Model GSF-5720G flow-through electrode, both from DKK-TOA Co. (Tokyo, Japan). The lysine composition was determined by collecting samples with an ADVANTEC Model CHF122SB fraction collector and analyzing them by HPLC as described previously.

THEORY

Ion Exchange Equilibria

As shown in our prior work (2–4), uptake of lysine by cation exchange resins, in general, results from the simultaneous exchange of monovalent and divalent lysine cations. Thus, both solution dissociation and ion exchange equilibria have to be considered. Lysine dissociates in solution according to:

$$AH_3^{2+} \Leftrightarrow AH_2^{+} + H^{+} \quad (1)$$

$$AH_2^{+} \Leftrightarrow AH^{\pm} + H^{+} \quad (2)$$

$$AH^{\pm} \Leftrightarrow A^{-} + H^{+} \quad (3)$$

where:

$$K_1 = \frac{C_{AH_2^+} C_{H^+}}{C_{AH_3^{2+}}} \tag{4}$$

$$K_2 = \frac{C_{AH^\pm} C_{H^+}}{C_{AH_2^+}} \tag{5}$$

$$K_3 = \frac{C_{A^-} C_{H^+}}{C_{AH^\pm}} \tag{6}$$

are the apparent dissociation constants. In our case, we consider a system that along with lysine also contains ammonia with chloride and sulfate as co-ions. Two additional dissociations need to be considered:

$$NH_4^+ \leftrightarrow NH_3 + H^+ \tag{7}$$

$$HSO_4^- \leftrightarrow SO_4^{2-} + H^+ \tag{8}$$

with:

$$K_N = \frac{C_{NH_3} C_{H^+}}{C_{NH_4^+}} \tag{9}$$

$$K_{S2} = \frac{C_{SO_4^{2-}} C_H^+}{C_{HSO_4^-}} \tag{10}$$

In principle, dissociation of H_2SO_4 into HSO_4^- could also be considered. In practice, however, the concentration of undissociated H_2SO_4 is negligible except at very high concentrations, which are beyond the scope if this work.

In general, these constants are related to the corresponding thermodynamic, infinite dilution values, K_i^T, by

$$K_1 = K_1 \frac{\gamma_{AH_2^+} \gamma_{H^+}}{\gamma_{AH_3^{2+}}} \tag{11}$$

$$K_2 = K_2 \frac{\gamma_{AH^\pm} \gamma_{H^+}}{\gamma_{AH_2^+}} \tag{12}$$

$$K_3 = K_3 \frac{\gamma_{A^-} \gamma_{H^+}}{\gamma_{AH^\pm}} \tag{13}$$

where the γ_i's are activity coefficients. The latter are functions of ionic strength, I, and can be expressed using the Davies equation (7). Accordingly

$$\log \gamma_i = -z_i^2 \left(\frac{A\sqrt{I}}{1+\sqrt{I}} - bI \right) \tag{14}$$

where z_i is the ion charge. A is the Debye-Hückel parameter (8), and can be estimated from

$$A = 1.8252 \times 10^6 \left(\frac{\rho_W}{\varepsilon^3 T^3}\right)^{1/2} \tag{15}$$

where ρ_W and ε are the density [g/cm^3] and dielectric constant of water, respectively. The latter is expressed as a function of temperature by the equation (9)

$$\varepsilon = \frac{5321}{T} + 233.76 - 0.9297T + 1.417 \times 10^{-3} T^2 - 8.292 \times 10^{-7} T^3 \tag{16}$$

while ρ_W is readily available in standard handbooks. Finally, the parameter b in Eq. (14) was taken to be 0.1 as suggested by (7).

Combining Eqs. (4–6), (11–13) and (14) yields the following relationships:

$$pK_1 = pK_1^T + 2\left(\frac{A\sqrt{I}}{1+\sqrt{I}} - bI\right) \tag{17}$$

$$pK_2 = pK_2^T \tag{18}$$

$$pK_3 = pK_3^T - 2\left(\frac{A\sqrt{I}}{1+\sqrt{I}} - bI\right) \tag{19}$$

The pK_i^T values of lysine were determined by (6) and depend on temperature according to the equation:

$$pK_i^T = \frac{1}{2.30}\left(\frac{\Delta H_{T,i}^0}{RT} + d_i\right) \tag{20}$$

with the values of $\Delta H_{T,i}^0$ and d_i summarized in Table 1. Note that pK_1^T is essentially independent of temperature while pK_2^T and pK_3^T decrease as temperature is increased.

Table 1. Constants for Eq. (20) and pK-values at different temperatures

	$\Delta H_{\mathrm{T,i}}^0/R$ $(K)^a$	$d_i{}^a$	25°C	40°C	60°C
pK_1^T	40	4.12	1.85	1.85	1.84
pK_2^T	4730	5.00	9.09	8.73	8.34
pK_3^T	5230	7.31	10.90	10.32	10.04
$pK_W^{T\,b}$	—	—	13.99	13.54	13.03
$pK_N^{T\,b}$	—	—	9.245	8.805	8.284
$pK_{S2}^{T\,b}$	—	—	1.987	2.170	2.310

[a](6).
[b](10).

In general, ion exchange equilibria can be described by the mass action law, using empirically determined equilibrium constants (11). For our system we have:

$$K_{Lys^{2+},H^+} = \frac{q_{Lys^{2+}} C_{H^+}^2}{q_{H^{+2}} C_{Lys^{2+}}} \tag{21}$$

$$K_{Lys^{+},H^+} = \frac{q_{Lys^{+}} C_{H^+}}{q_{H^+} C_{Lys^{+}}} \tag{22}$$

$$K_{NH_4^+,H^+} = \frac{q_{NH_4^+} C_{H^+}}{q_{H^+} C_{NH_4^+}} \tag{23}$$

where the q_i's are the resin-phase concentrations. Assuming complete exclusion of the co-ions, these concentrations are subject to the electroneutrality condition:

$$q_0 = 2q_{Lys^{2+}} + q_{Lys^{+}} + q_{NH_4^+} + q_{H^+} \tag{24}$$

Given the concentrations of total lysine ($C_L = C_{Lys^{2+}} + C_{Lys^{+}} + C_{Lys^{\pm}} + C_{Lys^{-}}$), total ammonia ($C_N = C_{NH_3} + C_{NH_4^+}$), chloride ($C_{Cl^-}$), and total sulfate ($C_s = C_{SO_4^{2-}} + C_{HSO_4^-}$, calculation of the resin composition from Eqs. (21–23) requires the concentrations of the individual ionic species. This is done by first calculating the solution pH by imposing the electroneutrality condition:

$$\begin{aligned} f = (2C_{Lys^{2+}} + C_{Lys^{+}} + C_{NH4^{+}} + C_{H^+}) - (C_{Lys^-} + C_{Cl^-} \\ + 2C_{SO_4^{2-}} + C_{HSO_4^-} + C_{OH^-}) = 0 \end{aligned} \tag{25}$$

combined with Eq (17–19) and the relationship $K_W = C_{H^+}\ C_{OH^-}$, this equation can be solved numerically for C_{H^+} from which $pH = -\log(\gamma_{H^+}\ C_{H^+})$. The concentrations of the individual ionic species can then be calculated from Eqs. (4–6) and (9–10). The values of pK_W, pK_N, and pK_{S2} needed for these calculations were obtained from the literature as summarized in Table 1. The ion exchange equilibrium constants were determined by fitting the equilibrium model to the experimental data for the NH_4^+/H^+, Lys^+/NH_4^+ and Lys^{2+}/H^+ exchanges. The Lys^+/NH_4^+ equilibrium constant was converted into Lys^+/H^+ equilibrium constant dividing it by the NH_4^+/H^+ equilibrium constant.

Ion Exchange Kinetics

The kinetics of ion exchange of amino acids is generally controlled by diffusion in the resin phase (11–14). This is also the case for lysine owing to its relatively bulky side chain (2). Batch adsorption experiments

were thus used to determine the relevant diffusion coefficients at different temperatures. Diffusional mass transfer within ion exchange particles can be described in terms of the Nernst-Planck equations. The complete set of equations is given in (2) and only a brief summary is presented here. The following equations and boundary conditions are written:

For the resin beads

$$\frac{\partial q_L}{\partial t} = -\frac{1}{r^2}\frac{\partial}{\partial r}\left[r^2\left(J_{Lys^+} + J_{Lys^{2+}}\right)\right] \tag{26}$$

$$\frac{\partial q_N}{\partial t} = -\frac{1}{r^2}\frac{\partial}{\partial r}\left[r^2\left(J_{NH_4^+} + J_{NH_3}\right)\right] \tag{27}$$

$$r = 0, \quad \frac{\partial q_L}{\partial r} = \frac{\partial q_N}{\partial r} = 0 \tag{28}$$

$$r = r_p, \quad q_L = q_L^*, \quad q_N = q_N^* \tag{29}$$

$$t = 0, \quad q_L = q_L^0, \quad q_N = q_N^0 \tag{30}$$

For the solution

$$\frac{d\bar{q}_L}{dt} = -\frac{V}{M_r}\frac{dC_L}{dt} = \frac{3}{r_p}\left(J_{Lys^{2+}} + J_{Lys^+}\right)\Big|_{r=r_p} \tag{31}$$

$$\frac{d\bar{q}_N}{dt} = -\frac{V}{M_r}\frac{dC_N}{dt} = \frac{3}{r_p}\left(J_{NH_4^+} + J_{NH_3}\right)\Big|_{r=r_p} \tag{32}$$

$$t = 0, \quad C_L = C_L^0, \quad C_N = C_N^0 \tag{33}$$

where $q_L = q_{Lys^+} + q_{Lys^{2+}}$ and $q_N = q_{NH_4^+} + q_{NH_3}$. In these equations, r_p is the particle radius, q_i^* is the equilibrium resin composition, q_i^0 is the initial resin composition, M_r is the mass of resin, V is the solution volume, and C_L^0 and C_N^0 are the initial lysine and ammonia solution concentrations, respectively. Equations (31–33) are obtained from material balances relating the concentrations averaged over the particle volume, $\bar{q}$, to the mass transfer fluxes at the particle surface. The fluxes are given by (14):

$$J_i = -\frac{1}{z_i}\sum_j z_j D_{i,j}\frac{\partial q_j}{\partial r} \tag{34}$$

where z_i is the ion charge and, M is the number of counterions and

$$D_{i,j} = -\frac{D_i(D_j - D_M)z_i^2 q_i}{\sum_{k=1}^{M} z_k^2 D_k q_k} \quad \text{for } i \neq j \tag{35}$$

$$D_{i,i} = D_i - \frac{D_i(D_i - D_M)z_i^2 q_i}{\sum_{k=1}^{M} z_k^2 D_k q_k} \quad \text{for } i = j \tag{36}$$

where D_i is the resin phase diffusivity of ion i, D_M is the diffusivity of a reference ion, H^+, in our case. In addition to these equations the following relationship also exist between monovalent and divalent forms of lysine and free ammonia and ammonium ion:

$$K_1^R = \frac{q_{Lys^+} q_{H^+}}{q_{Lys^{2+}}} \tag{37}$$

$$K_N^R = \frac{q_{NH_3} q_{H^+}}{q_{NH_4^+}} \tag{38}$$

where $K_1^R = K_1(K_{Lys^+,H^+}/K_{Lys^{2+},\ H^+})$ and $K_N^R = K_N\,(K_p/K_{H^+}{}^{NH_4^+})$ are the resin-phase dissociation constants for divalent lysine and ammonium ion, respectively. K_p is the partition coefficient for free ammonia (NH_3) in the resin. The value $K_p = 0.68 \pm 0.01$ as determined by (13). The resulting equations were solved numerically as discussed in (2).

Prediction of Column Behavior

The behavior of a resin column can be predicted starting with the following material balances:

$$\rho_b \frac{\partial \bar{q}_L}{\partial t} + \varepsilon \frac{\partial C_L}{\partial t} + u \frac{\partial C_L}{\partial z} = 0 \tag{39}$$

$$\rho_b \frac{\partial \bar{q}_N}{\partial t} + \varepsilon \frac{\partial C_N}{\partial t} + u \frac{\partial C_N}{\partial z} = 0 \tag{40}$$

$$\varepsilon \frac{\partial C_S}{\partial t} + u \frac{\partial C_S}{\partial z} = 0 \tag{41}$$

$$\varepsilon \frac{\partial C_{Cl^-}}{\partial t} + u \frac{\partial C_{Cl^-}}{\partial z} = 0 \tag{42}$$

$$t = 0,\ C_L = C_L^0,\ C_N = C_N^0,\ C_S = C_S^0,\ C_{Cl^-} = C_{Cl^-}^0 \tag{43}$$

$$z = 0,\ C_L = C_L^F,\ C_N = C_N^F,\ C_S = C_S^F,\ C_{Cl^-} = C_{Cl^-}^F \tag{44}$$

where u is the superficial velocity, ρ_b is the bed resin density, ε is the void fraction, and superscript F and 0 refer to feed and initial conditions, respectively. These equations assume plug flow and neglect axial dispersion, which is appropriate for preparative-scale resins where band broadening is controlled by intraparticle diffusion. In principle, these equations can be combined with Eqs. (27–27) and (34–36). In practice, however, sufficient accuracy is obtained with a simplified description in terms of the film model

approximation of (15). The following rate equations are obtained (3):

$$\frac{\partial \bar{q}_{Lys^+}}{\partial t} = \frac{3D_{Lys^+}}{r_p^2} m \frac{\overline{q}_{Lys^+} - q^*_{Lys^+} e^{m/5}}{1 - e^{m/5}} \tag{45}$$

$$\frac{\partial \bar{q}_{Lys^{2+}}}{\partial t} = \frac{3D_{Lys^{2+}}}{r_p^2} 2m \frac{\overline{q}_{Lys^{2+}} - q^*_{Lys^{2+}} e^{m/5}}{1 - e^{m/5}} \tag{46}$$

$$\frac{\partial \bar{q}_{NH_4^+}}{\partial t} = \frac{3D_{NH_4^+}}{r_p^2} m \frac{\overline{q}_{NH_4^+} - q^*_{NH_4^+} e^{m/5}}{1 - e^{m/5}} \tag{47}$$

$$\frac{\partial \bar{q}_{NH_3}}{\partial t} = \frac{15D_{NH_3}}{r_p^2} (q^*_{NH_3} - \overline{q}_{NH_3}) \tag{48}$$

where the overbar represents the average resin composition. The parameter m is determined by solving the equation (4):

$$\sum_{j=1}^{M} \left(z_j^2 D_j \frac{\bar{q}_j - q_j^* e^{m z_j/5}}{1 - e^{m z_j/5}} \right) = 0 \tag{49}$$

These equations are solved numerically with backwards discretization of the spatial derivative using 10 finite difference points (3).

RESULTS

Ion Exchange Equilibria

Ion exchange equilibrium data were obtained for the binaries NH_4^+/H^+, Lys^{2+}/H^+, and Lys^+/NH_4^+ and are shown in Figs. 1–3. For each binary the temperature dependence of the ion exchange equilibrium appears to be insignificant. Thus the equilibrium constants $K_{NH_4^+,H^+}$, K_{Lys^{2+},H^+}, K_{Lys^+,NH_4^+}, are invariant with temperature and were determined by fitting Eq. (21–23) to the data. The resulting values are summarized in Table 2. For the NH_4^+/H^+ and Lys^{2+}/H^+ exchange equilbria, concentration-independent values of $K_{NH_4^+,H^+}$, and K_{Lys^{2+},H^+}, provide good fits of the data (see Fig. 1 and 2). However, this is not the case for the Lys^+/NH_4^+ equilibrium. For this exchange, following (2) we use a heterogeneous ion exchange model assuming that exchange occurs on two types of functional groups. Accordingly, for each functional group we have:

$$K^j_{i,H^+} = \frac{q^j_i (C_{H^+})^{z_i}}{(q^j_{H^+})^{z_i} C_i} \tag{50}$$

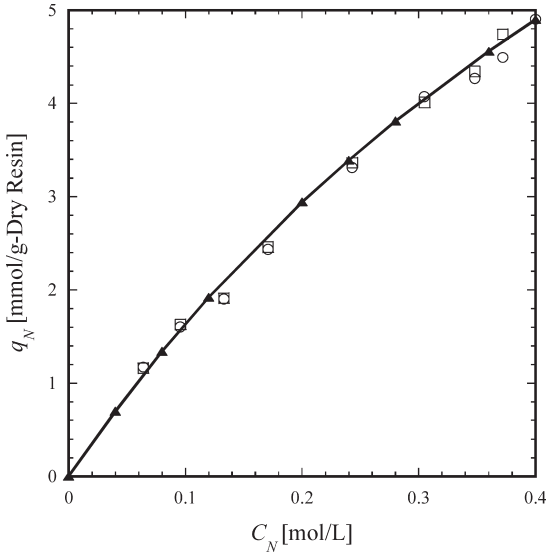

Figure 1. NH_4^+/H^+ ion exchange equilibrium with $C_N^0 = 0.40$ M and $C_{Cl^-} = 0.40$ M. Line is based on $K_{NH_4^+,H^+} = 1.5$. Symbols are 25°C (○), 40° C(□) and 60°C (▲).

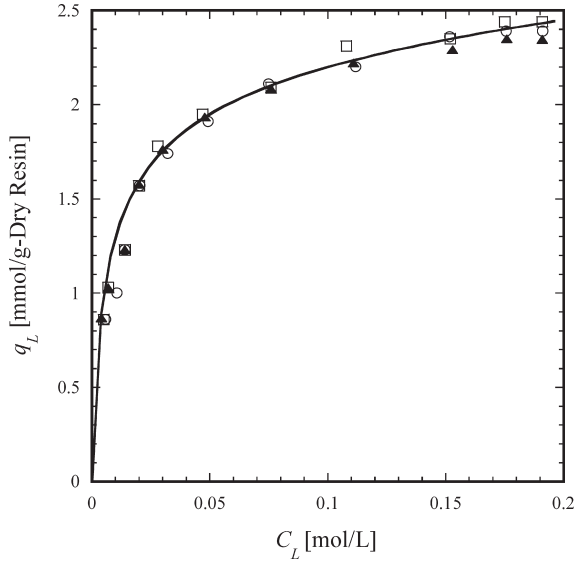

Figure 2. Lys^{2+}/H^+ ion exchange equilibrium with $C_L^0 = 0.20$ M and $C_{Cl^-} = 0.35$ M. Line is based on $K_{Lys^{2+},H^+} = 6.0\ g/cm^3$. Symbols are 25°C (○), 40°C (□) and 60°C (▲).

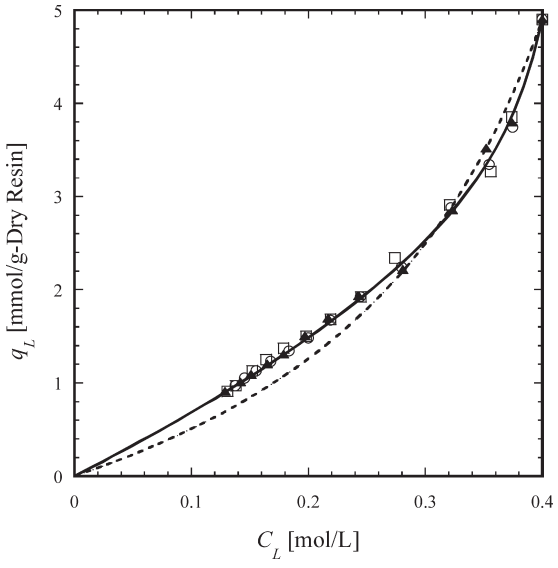

Figure 3. Lys^+/NH_4^+ ion exchange equilibrium with $C_L^0 = 0.40$ M and $C_{Cl^-} = 0.40$ M. Solid line is based on the heterogeneous ion exchange model with $p_1 = 0.6$, $K^1_{Lys^+,H^+} = 1.20$, $K^2_{Lys^+,H^+} = 0.15$. Dashed line is based on homogenous ion exchange model with $K_{Lys^+,H^+} = 0.52$. Symbols are 25°C (○), 40°C (□) and 60°C (▲).

subject to the constraint:

$$q_0^j = p_j q_0 = \sum_i z_i q_i^j \tag{51}$$

where K^{d}_{i,H^+} is equilibrium constant for exchange of ion i and H^+ on group j, z_i is the charge of ion I, and p_j is the fraction of groups that are of type j. The average equilibrium constant $\bar{K}_{i,H^+}$ is related to the values for each group

Table 2. Ion exchange equilibrium constants for monovalent and divalent lysine cations and ammonium ion in heterogeneous ion exchange model with $p_1 = 0.6$. The values given are independent of temperature

	DIAION SK 1B			Dowex HCR-W2[a]		
Component, i	$\bar{K}_{i,H^+}$	K^1_{i,H^+}	K^2_{i,H^+}	$\bar{K}_{i,H^+}$	K^1_{i,H^+}	K^2_{i,H^+}
Lys^{2+} [g/cm^3]	6.0	6.0	6.0	5.0	5.0	5.0
Lys^+ [−]	0.52	1.2	0.15	0.75	1.5	0.27
NH_4^+ [−]	1.5	1.5	1.5	1.5	1.5	1.5

[a]From (2) at 25°C.

type through the following equation (16):

$$\bar{K}_{i,H^+} = (K^1_{i,H^+})^{p_1}(K^2_{i,H^+})^{1-p_1} \tag{52}$$

The best fit of the Lys^+/NH_4^+ data was obtained with $p_1 = 0.6$, $K^1_{Lys^+,H^+} = 1.20$ and $K_{Lys^+,H^+} = 0.15$.

The equilibrium constants determined in this work for the DIAION SK1B resin are compared with the values previously reported by (2) for Dowex HCR-W2 in Table 2. Both resins are nominally 8% crosslinked. K-values are the same for the ammonium-hydrogen ion exchange, but they are similar for the divalent lysine-hydrogen and monovalent lysine-hydrogen exchanges indicating that the two resins are comparable.

Resin Phase Diffusivities

Batch ion exchange kinetics data were obtained for the binaries NH_4^+/H^+, Lys^{2+}/H^+, and Lys^+/NH_4^+. Representative results obtained at 25 and 60°C with different amounts of resin are shown in Figs. 4–6. Results at 40°C were intermediate (data not shown). It can be seen that the kinetics is fastest for the NH_4^+/H^+ exchange and slowest for the Lys^{2+}/H^+ exchange. In all three cases, however, the kinetics is improved dramatically by increasing the temperature from 25 to 60°C. As discussed in the Theory section, the mass transfer fluxes are electrically coupled. Thus, individual ion diffusivities were determined by fitting model calculations based on Eq. (26–36) to the data with the following methodology. The diffusivity of hydrogen ion in 8% crosslinked resins, D_{H^+}, is available at 25°C (17).Thus, $D_{NH_4^+}$ can be obtained at this temperature by fitting the model to the data in Fig. 4a. For the other temperatures, we assumed that the ratio $D_{NH_4^+}/D_{H^+}$ remains constant. This assumption is valid for diffusion in the liquid phase 18 and is likely to apply to the resin phase as well. Next we determined the divalent and monovalent lysine diffusivities from the data in Figs. 5 and 6, respectively, using the $D_{NH_4^+}$ - value determined at each temperature. Here both $D_{Lys^{2+}}$ and D_{Lys^+} are so small that the much larger hydrogen ion diffusivity plays almost no role in the overall kinetics. Thus, for these conditions, mass transfer is largely controlled by $D_{Lys^{2+}}$ and D_{Lys^+}. As a result these values can be determined accurately from the data in Figs. 5 and 6.

A summary of the diffusivity values is given in Table 3. Diffusivities of all species increase dramatically as the temperature is increased. This behavior is compared with the results for phenylalanine of (5) and with the diffusivities in the solution phase predicted by using Wilke-Chang equation (18) in Fig. 7. It can be seen that the effect of the temperature on the resin-phase diffusivity for both mono- and divalent lysine cations is similar to that of phenylalanine cations and is much more pronounced than the effect predicted for the

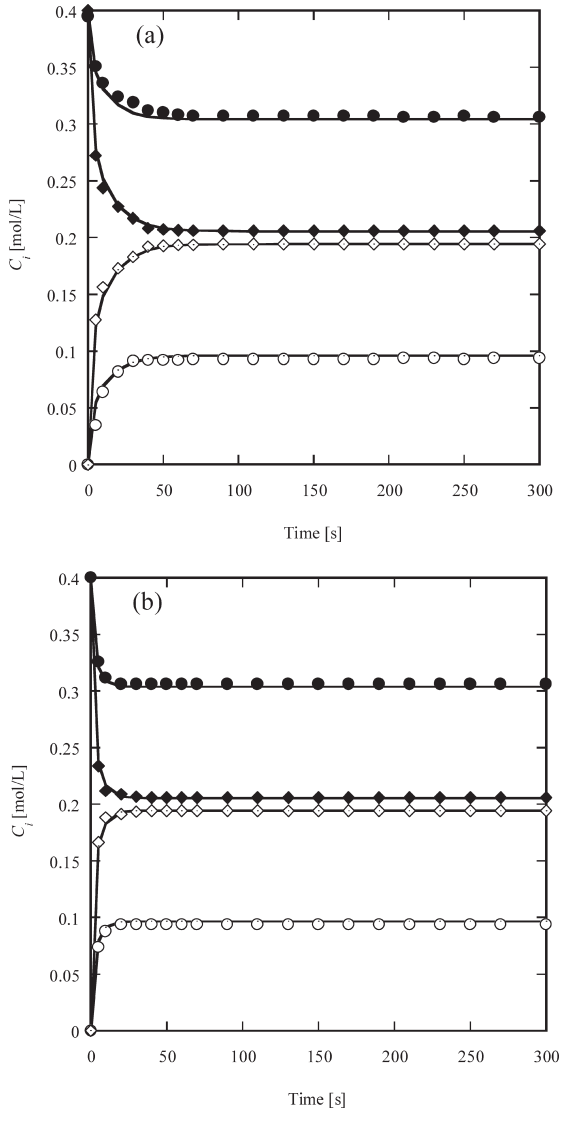

Figure 4. Batch uptake of NH_4^+ by H^+-form resin with $C_{NH_4^+} = 0.40$ M,$C_{Cl}^- = 0.40$ M at (a) 25°C, and (b) 60°C. Lines are based on the Nernst-Plank model. Symbols: Hydrogen ion (○) and total ammonia (●) with $M_r = 2.4$ g. Hydrogen ion (◇) and total ammonia (◆) with $M_r = 6.5$ g.

solution phase. Thus, increasing the temperature enhances the ion exchange kinetics much more than could be expected for transport in free solution. The monovalent lysine diffusivity is larger than that of phenylalanine, likely because of the bulkier hydrophobic side chain of the latter amino acid.

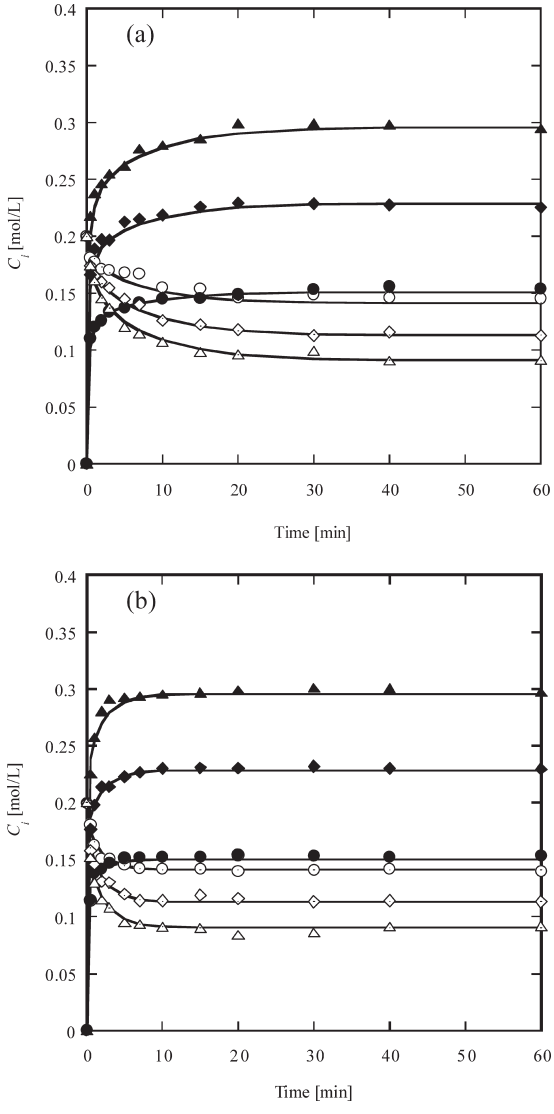

Figure 5. Batch uptake of Lys^{2+} by NH_4^+ form resin with $C_L^0 = 0.20$ M,$C_{Cl}^- = 1.00$ M at (a) 25°C and (b) 60°C. Lines are based on Nernst-Plank model. Symbols: total lysine (○) and total ammonia (●) with $M_r = 3.4$ g. Total lysine (◇) and total ammonia (◆) with $M_r = 5.5$ g; total lysine (△) and total ammonia (▲) with$M_r = 7.6$ g.

Finally, divalent lysine cations have even lower resin phase diffusivity. This trend is also seen when comparing monovalent and divalent inorganic cations and is likely a result of the stronger interaction of divalent cations with the resin's charged groups.

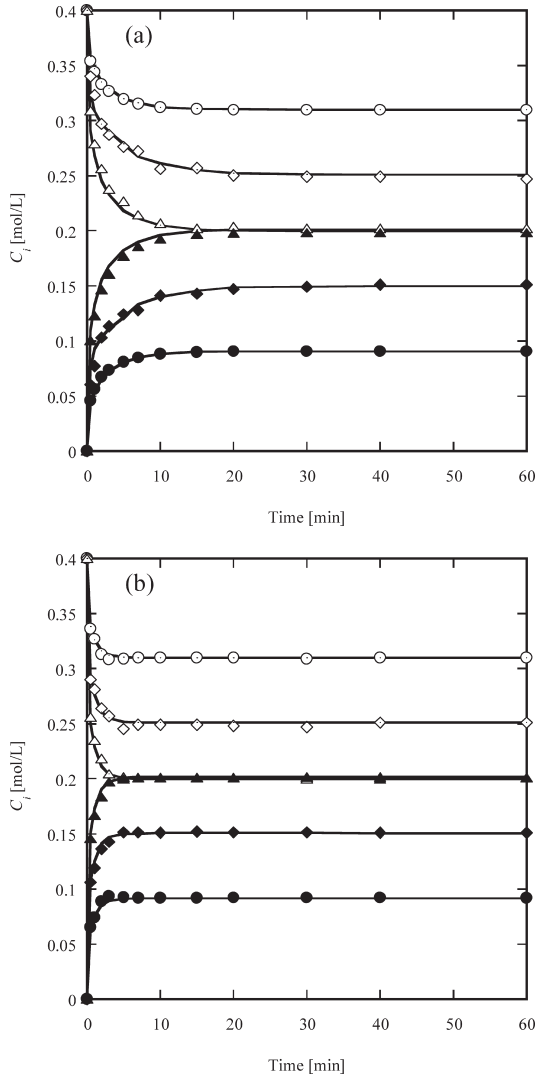

Figure 6. Batch uptake of Lys^+ by NH_4^+-form resin with $C_L^0 = 0.40$ M,$C_{Cl}^- = 0.40$ M at (a) 25°C and (b) at 60°C. Lines are based on Nernst-Plank model. Symbols: Total lysine (○) and total ammonia (●) at $M_r = 3.4$ g; total lysine (◇) and total ammonia (◆) at$M_r = 7.6$ g; total lysine (△) and total ammonia (▲) at$M_r = 13.6$ g.

Column Behavior

Experimental results for column adsorption and desorption of lysine at 25 and 60°C are shown in Figs. 8 and 9 with a 0.2 M lysine feed contain 0.1 M and 0.4 M total sulfate, respectively. In both cases, desorption was with 1.0 M

Table 3. Resin phase ion diffusivities in DIAION SK1B at 25°C, 40°C, and 60°C. Values are given in 10^{-6} cm^2/s

Species	25°C	40°C	60°C
Lys^{2+}	0.04	0.08	0.14
Lys^{+}	0.16	0.32	0.55
NH_4^+	1.8	3.0	6.0
H^+	12	20	40

ammonium hydroxide. The first case, Fig. 8, corresponds to conditions where lysine is predominately in monovalent form during the adsorption step, since the pH is relatively high. For these conditions, lysine adsorption is thermodynamically unfavorable (see Fig. 2) and the breakthrough curve follows a gradual wave pattern. In this case, temperature has a small effect since band broadening is dominated by the unfavorable nature of the Lys^+/NH_4^+ exchange. The effect of temperature is however much more pronounced for the desorption step. In 1.0 M ammonium hydroxide, the lysine is completely deprotonated and carries a negative charge. As a result it is completely excluded from the resin making the desorption process entirely diffusion

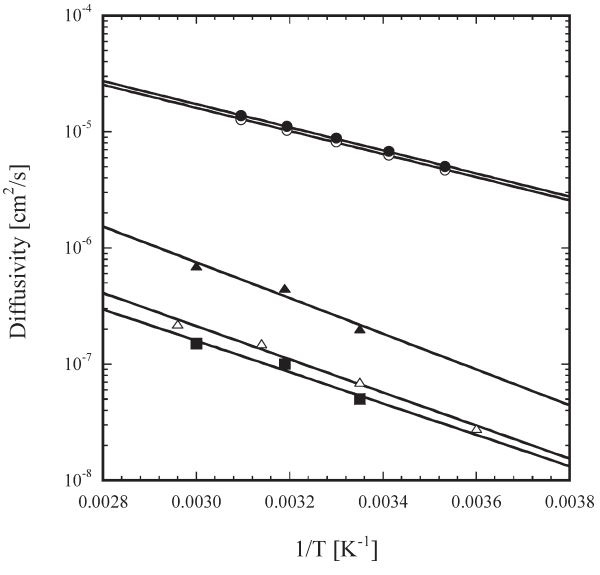

Figure 7. Resin phase diffusivities of lysine and phenylalanine in water and in the resin used in this study as a function of temperature. The phenylalanine values are from Borst et al. 1997. Symbols are phenylalanine in water (○), phenylalanine in Dowex HCR-W2 (△), lysine in water (●), monovalent lysine in DIAION SK1B (▲) and divalent lysine in DIAION SK1B (■).

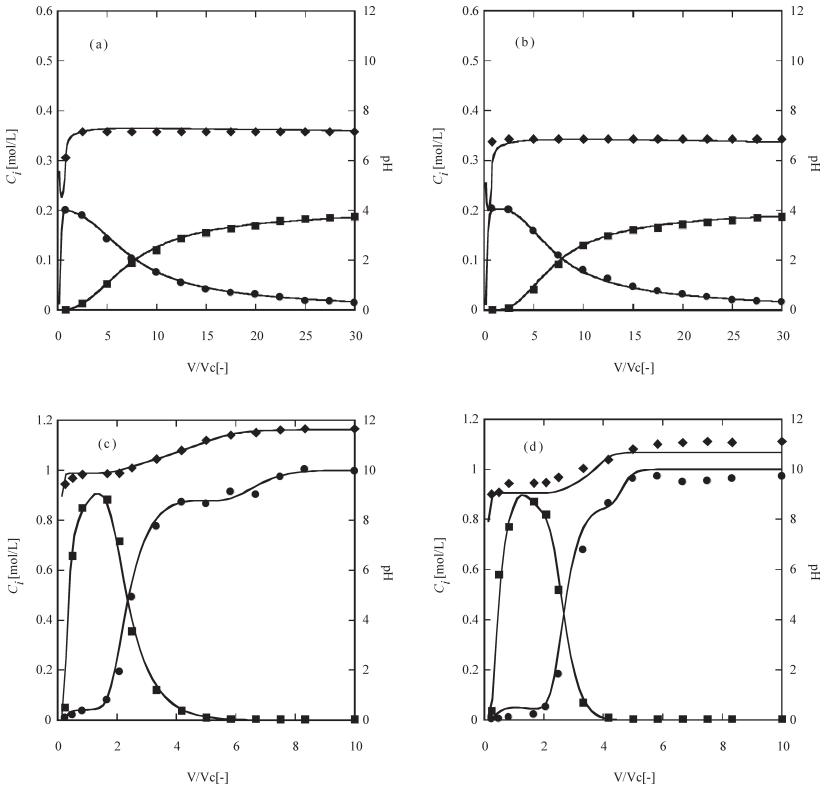

Figure 8. Column adsorption (a and b) $C_L^0 = 0.20$ M, $C_S^0 = 0.10$ M and desorption (c and d) desorption with 1.0 M NH_4OH at 25°C. (a and c) and 60°C (b and d). $L = 5.0$ cm, $u = 0.00694$ cm/s. Symbols are total ammonia (●), total lysine (■) and pH (◆).

controlled. As seen by comparing Figs. 8c and d, the tailing of the lysine desorption curve is greatly reduced at 60°C, resulting in a more efficient process. Correspondingly the height of the desorption peak is increased. Intermediate results were obtained at 40°C (data not shown). Model predictions, based on the equilibrium constants and diffusivities determined in this work are also shown in Figs. 8 and 9 and are in excellent agreement with the experimental results.

The results shown in Fig. 9 are for conditions where the lysine is predominately in divalent form during the adsorption step because of the relatively low pH. In this case, the breakthrough curve follows a shock pattern and band broadening is controlled by mass transfer. As seen in Figs. 9a and b, the position of the breakthrough patterns does not change with temperature, since the uptake equilibrium is invariant. However, the curve becomes significantly sharper as a results of the higher resin phase diffusivity when the

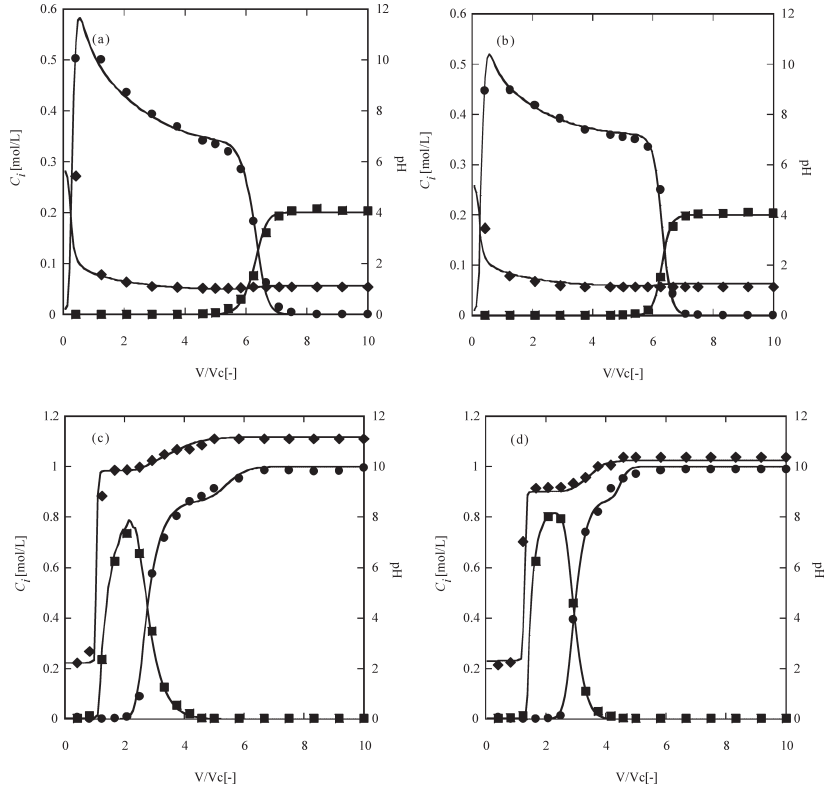

Figure 9. Column adsorption (a and b) $C_L^0 = 0.20$ M, $C_S^0 = 0.40$ M and desorption (c and d) desorption with 1.0 M NH_4OH at 25°C. (a and c) and 60°C (b and d). $L = 5.0$ cm, $u = 0.00347$ cm/s. Symbols are total ammonia (●), total lysine (■) and pH (◆).

temperature is increased from 25 to 60°C. Substantial improvements are also seen for the desorption curves (Figs. 9c and d) with significant reduction in tailing and higher peak concentrations when the temperature is increased from 25 to 60°C. Intermediate results were found at 40°C (data not shown). As for the intermediate pH cases, model predictions are also in excellent agreement with the data supporting the validity of the model and the experimental determinations of ion exchange equilibrium constants and diffusivities.

CONCLUSIONS

Ion exchange equilibrium and kinetics were determined for lysine adsorption on a cation exchange resin at temperatures of 25, 40, and 60°C. Increasing

temperature was found to have insignificant effects on ion exchange equilibrium but to enhance dramatically the exchange kinetics. A model taking into account the solution equilibrium was used to determine the ion exchange equilibrium constants for ammonium ion and for monovalent and divalent lysine. These constants are essentially independent of temperature. Resin phase diffusivities were found by fitting batch ion exchange data and exhibit an Arrenhius-type dependence on temperature with an activation energy about twice as large as that predicted for diffusion in free solution. Finally, the modeling approach and the physical constants obtained in this work were validated by comparing experimental column adsorption and desorption results with predictions based on a model incorporating solution and ion exchange equilbria and diffusional mass transfer kinetics. Excellent agreement between model and data supports the validity of the overall approach. An important conclusion is based on the result that the lysine adsorption capacity does not change with temperature while the resin phase diffusivities increase dramatically as the temperature is increased from 25 to 60°C. This behavior can be exploited in a process to increase the dynamic binding capacity and the concentration of the desorbed product while reducing the consumption of the desorbent as a result of the much less pronounced tailing obtained at higher temperatures.

REFERENCES

1. Blanch, H.W. and Clark, D.S. (1997) *Biochemical Engineering*; Marcel-Dekker, Inc.,: New York.
2. Nagai, H. and Carta, G. (2004a) Lysine adsorption on cation exchange resin I. Ion exchange equilibrium and kinetics. *Sep. Sci. Technol.*, 39: 3691–3710.
3. Nagai, H. and Carta, G. (2004b) Lysine adsorption on cation exchange resin II. Column adsorption/desorption behavior and modeling. *Sep. Sci. Technol.*, 39: 3711–3738.
4. Nagai, H. and Carta, G. (2005) Lysine adsorption on cation exchange resin III. Multicolumn adsorption/desorption operation. *Sep. Sci. Technol.*, 40: 791–809.
5. Borst, C.L., Grzegorczky, D.S., Strand, S.J., and Carta, G. (1997) Temperature effects on equilibrium and mass transfer of phenylalanine in cation exchangers. *Rect. & Func. Polymers.*, 32: 25–41.
6. Nagai, H., Kuwabara, K., and Carta, G. (2007) Temperature dependence of the dissociation constants of several amino acids. *J. Chem. Eng. Data*, submitted to.
7. Davies, C.W. (1962) *Ion Association*; Butterworths: London.
8. Debye, P. and Hückel, E. (1923) The theory of electrolytes. I. Lowering of freezing point and related phenomena. *Physik Z.*, 24: 185–206.
9. (a) Akerlof, G.C. and Oshry, H.I. (1950) The dielectric constant of water at high temperatures and in equilibrium with its vapor. *J. Am. Chem. Soc.*, 72 (7): 2844–2847; (b) John, A.D. (1985) *Lange's Handbook of Chemistry*, 13th Edn.; MacGraw-Hill: New York.
10. Lange, N.A. (1985) *Lange's Handbook of Chemistry, 13th Edition*; McGraw-Hill: New York.

11. Helfferich, F. (1962) *Ion Exchange*; Mcgraw-Hill: New York.
12. Saunders, S.M., Vierow, J.B., and Carta, G. (1989) Uptake of phenylalanine and tyrosine by a strong-acid cation exchanger. *AIChE J.*, 35: 53–68.
13. Jones, L.I. and Carta, G. (1993) Ion-exchange of amino acids and dipeptides on cation resins with varying degree of cross-linking 1. Equilibrium. *Ind. Eng. Chem. Res.*, 32: 117–125.
14. LeVan, M.D., Carta, G., and Yon, C. (1997) Adsorption and ion exchange, chapter 16. In *Perry's Chemical Engineers' Handbook*, 7th Edn.; Green, D.W. (ed.); McGraw-Hill: New York.
15. Carta, G. and Lewus, R.K. (1999) Film model approximation for particle-diffusioncontrolled multicomponent ion exchange. *Sep. Sci. Technol.*, 34: 2685–2697.
16. Melis, S., Cao, G., and Morbidelli, M. (1995) A new model for the simulation of ion exchange equilibria. *Ind. Eng. Chem. Reserch*, 34: 3916–3924.
17. Kataoka, T. and Yoshida, H. (1975) Resin phase mass transfer in ion exchange between different ions accompanied by resin volume change. *J. Chem. Eng. Jpn.*, 6: 451–456.
18. Cussler, E.L. (1997) *Diffusion-Mass Transfer in Fluid Systems*, 2nd Edn.; Cambridge University Press: Cambridge, United Kingdom.